DRAFT SF 298

1. Report Date (dd-mm-yy)	2. Report Type	3. Dates covered (from... to)

4. Title & subtitle The Use of Electrochemical Impedance Spectroscopy (EIS) and Electrochemical Noise Analysis (ENA) for Monitoring of Biocorrosion Tri-Service Committee on Corrosion Proceedings	5a. Contract or Grant #
	5b. Program Element #
6. Author(s) Dr. F. Mansfeld Mr. H. Xiao Mr. Y. Wang	5c. Project #
	5d. Task #
	5e. Work Unit #

7. Performing Organization Name & Address	8. Performing Organization Report #
9. Sponsoring/Monitoring Agency Name & Address Tri-Service Committee on Corrosion USAF WRIGHT-PATTERSON Air Force Base, Ohio 45433	10. Monitor Acronym
	11. Monitor Report #

12. Distribution/Availability Statement
Approved for Public Release
Distribution Unlimited

13. Supplementary Notes

14. Abstract

15. Subject Terms
Tri-Service Conference on Corrosion

Security Classification of			19. Limitation of Abstract	20. # of Pages	21. Responsible Person (Name and Telephone #)
16. Report	17. Abstract	18. This Page			

TRI-SERVICE CONFERENCE ON CORROSION

21-23 JUNE 1994

SHERATON PLAZA HOTEL
ORLANDO, FLORIDA

PROCEEDINGS

THE USE OF ELECTROCHEMICAL IMPEDANCE SPECTROSCOPY (EIS) AND ELECTROCHEMICAL NOISE ANALYSIS (ENA) FOR MONITORING OF BIOCORROSION

Dr. F. Mansfeld*, Mr. H. Xiao and Mr. Y. Wang
Corrosion and Environmental Effects Laboratory (CEEL)
Department of Materials Science and Engineering
University of Southern California
Los Angeles, CA 90089-0241

Abstract

The use of electrochemical impedance spectroscopy (EIS) and electrochemical noise analysis (ENA) for non-destructive evaluation of corrosion processes is illustrated for three model systems. EIS can be used to detect and monitor localized corrosion of Al alloys and determine pit growth laws which can be used for lifetime prediction purposes. Electrochemical potential and current noise data can be analyzed in the time and the frequency domain. A comparison of noise data obtained for Pt and an Al 2009/SiC metal matrix composite (MMC) exposed to 0.5 N NaCl has shown that the use of potential noise data alone can lead to misleading results concerning corrosion kinetics and mechanisms. The electrochemical noise data have been evaluated using power spectral density (PSD) plots in an attempt to obtain mechanistic information. The system Fe/NaCl has been used to determine the relationship between the polarization resistance R_p obtained from EIS data and the noise resistance R_n determined by statistical analysis of potential and current noise data. Potential and current noise can be recorded simultaneously allowing construction of noise spectra from which the spectral noise resistance R^o_{sn} can be obtained as the limit for zero frequency. Good agreement between R_p, R_n and R^o_{sn} has been observed for iron exposed to NaCl solutions of different corrosivity. For polymer coated steel exposed to 0.5 NaCl for five months analysis of EIS data allows to draw conclusions concerning the degree of disbonding of the coating and the decrease of the coating resistivity with exposure time. R_n and R^o_{sn} obtained from electrochemical noise data for an alkyd coating on cold rolled steel agree with each other and show the same time dependence as R_p and the pore resistance R_{po} determined from EIS data, but are significantly lower than R_p and R_{po}. The relationships of derived noise parameters such as R_n and R^o_{sn} to coating properties and to the remaining lifetime of a polymer coating are not clear at present.

Introduction

In evaluating the use of electrochemical monitoring techniques for the detection and quantification of microbiologically influenced corrosion (MIC), a few limitations of such techniques have to be considered. A weakness of most electrochemical techniques is the failure to give quantitative results in cases of localized corrosion. These techniques give average readings for the surface of a test electrode and it is not clear whether a measured corrosion current corresponds to uniform corrosion of the entire surface or to localized corrosion of just a few sites on this surface. In the latter case corrosion rates will be severely underestimated if the measured corrosion loss is not normalized to the area at which localized corrosion occurs - a quantity which is usually unknown. This general disadvantage of electrochemical techniques is especially bothersome in the case of MIC, where most corrosion processes are of a localized nature. Recently, techniques such as electrochemical impedance spectroscopy (EIS) have been shown to contain information which is specifically related to localized corrosion processes [1-4]. EIS can be considered a well-established technique in corrosion research which has been applied successfully in studies of many corrosion systems [4,5]. Due to the practical importance of localized phenomena in areas such as MIC, it is desirable to apply EIS to studies of pitting and crevice corrosion with the aim of quantifying these corrosion processes through measurements of pit growth rates and other parameters uniquely related to localized corrosion.

Another new technique is electrochemical noise analysis (ENA), which is considered by some as the ideal tool for the study of localized corrosion phenomena. ENA has the advantage that it is a non-destructive technique which monitors naturally occurring phenomena. No external signal has to be applied to collect noise data. Unfortunately, very few studies have demonstrated that localized corrosion can be detected and analyzed quantitatively by ENA for a system for which no previous information concerning its corrosion mechanism is available. So far ENA has been used mainly to detect the onset of localized corrosion and to monitor its progress in a qualitative manner. On-going work at CEEL is devoted to comparisons of information concerning types and rates of localized corrosion processes which can be obtained with EIS and ENA and to evaluate the use of ENA as a corrosion monitoring tool in applications such as MIC. In the following, the application of EIS and ENA to three corrosion systems will be discussed in order to demonstrate this approach. While the results discussed below have been obtained in abiotic solutions, they still illustrate the experimental approach taken in applications of EIS and ENA and form the basis of

future projects to be carried out by the authors in which these techniques will be applied in evaluation of MIC phenomena.

Experimental Results and Discussion

Materials and Methods

Materials and Test Solutions. In the study of pitting of Al-based materials impedance spectra were obtained for Al 6061 exposed to 0.5 N NaCl. Electrochemical noise data were determined for an Al 2009/SiC, T-8 metal matrix composite (MMC) containing 20% SiC particles and for pure Pt in the same solution. Comparison of EIS and ENA data for pure Fe (99.999 %) were carried out in three solutions of NaCl with different corrosivity. The study of polymer coated cold-rolled steel with EIS and ENA was carried out in 0.5 N NaCl for two different coating systems.

Methods. EIS data for Al 6061 were determined with a three-electrode system using Solartron model 1186 or 1286 potentiostats and a Solartron model 1250 frequency response analyzer (FRA). Impedance spectra were analyzed using the PITFIT software [6]. Potential and current noise data for Al 2009/SiC and pure Fe were determined sequentially for a two-electrode system using a Solartron model 1286 potentiostat as a ZRA and a HP model 3475A voltmeter. The noise data for Al 2009/SiC data were collected over a 4096 sec. time period with a sampling rate of 2 points/sec, while the data for pure Fe were collected during a 500 sec. time period. Noise data for pure Fe were also collected simultaneously using two digital voltmeters (HP 3457A and 3478A) and software developed at CEEL as described elsewhere [7,8]. The same technique was used for the evaluation of two polymer coatings on cold-rolled steel. EIS data were collected for the same two-electrode system after each noise measurement which was carried out for 1024 sec and a sampling rate of 2 points/sec.

1. Localized Corrosion of Al Alloys and Al-Based Metal Matrix Composites.

Mansfeld and co-workers have demonstrated that the pitting model shown in Fig. 1 can be used to determine pit growth rates from impedance spectra collected at the corrosion potential E_{corr} [6,9]. C_p and R_p refer to the passive surface, while C_{pit}, R_{pit} and W are properties of active pits. Fig. 2 shows experimental data for Al 6061 in the untreated condition (Fig. 2a and b) and after surface modification in the Ce-Mo Process which produces excellent resistance to localized corrosion (Fig. 2c) [10,11]. This is demonstrated by the capacitive nature of the Bode

plots in Fig. 2c, the very high values of R_p and the lack of change in the impedance data during exposure to 0.5 N NaCl for 30 days.

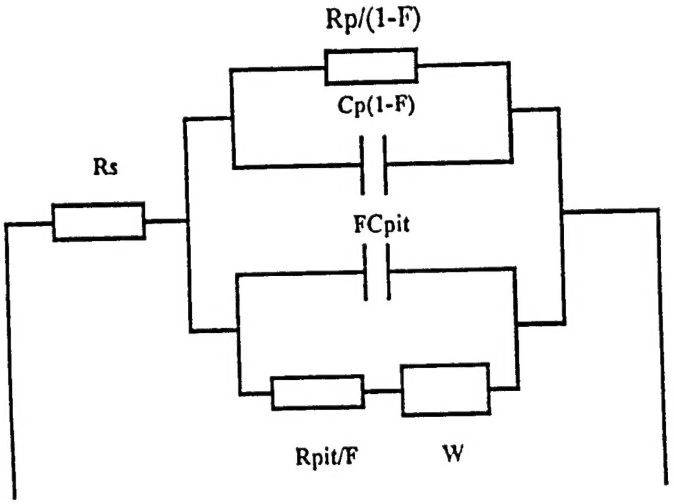

$0 \le F \le 1, W = (K/F)(j\omega)^n, n < 0$

Fig. 1. Pitting model for Al alloys

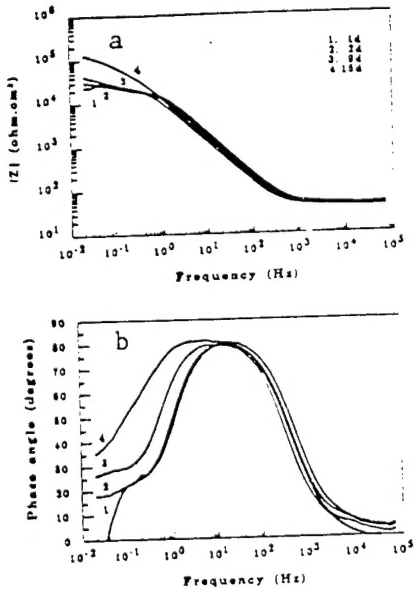

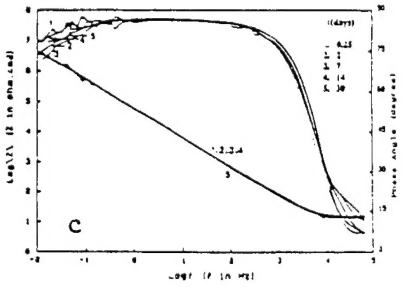

Fig. 2. Impedance spectra for untreated (Fig. 2a and b) and surface modified (Fig. 2c) Al 6061 with different exposure times in 0.5 N NaCl

Determination of pit growth rates for the untreated samples requires calculation of the specific pit polarization resistance $R^o_{pit} = R_{pit} \times A_{pit}$ from the fit parameter R_{pit} and the pitted area A_{pit} as a function of exposure time. $A_{pit} = 2FA$ is calculated from the time dependence of the area fraction F at which pitting occurs (Fig. 1) and the total area A assuming hemispherical pits [12]. Fig. 3 shows the time dependence of R_{pit} (Fig. 3 a) and A_{pit} (Fig. 3 b) for two samples of Al 6061 with different surface preparation (as-received vs. polished). Pit growth rates v_{pit} have been expressed as [11]:

$$v_{pit} = a(t - t_o)^b \qquad (1),$$

where t_o is the time at which pits were first observed and a and b are parameters which have to be determined experimentally.

Since v_{pit} is proportional to $1/R^o_{pit}$, Eq. 1 can be written as:

$$\log (1/R^o_{pit}) = \log a' + b \log (t - t_o) \qquad (2)$$

in order to apply the experimental impedance data, i.e. R^o_{pit}.

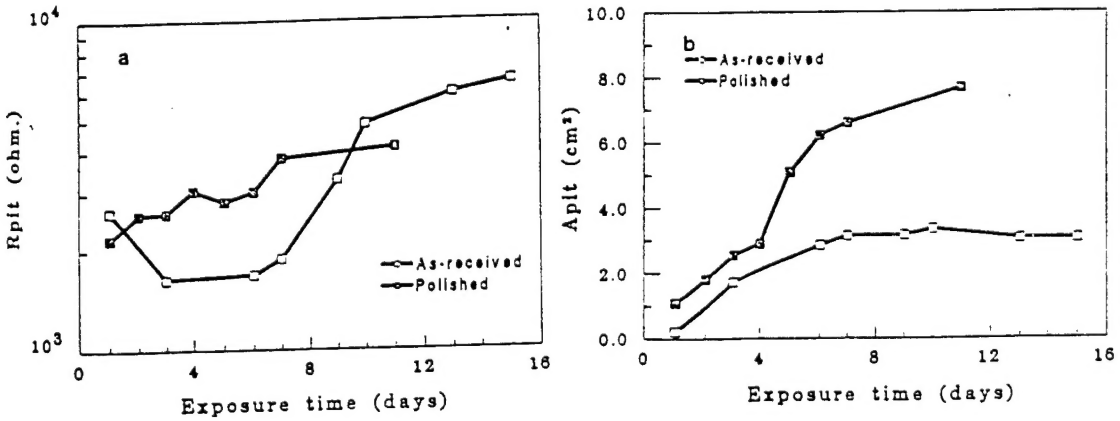

Fig. 3. Time dependence of R_{pit} (Fig. 3a) and A_{pit} (Fig. 3b) for untreated (as-received vs. polished) Al 6061 exposed to 0.5 N NaCl

Experimental results for Al 6061 based on the data in Fig. 3 are shown in Fig. 4, where pits originated during the first day of exposure (t_o < 1 day). Straight lines with a slope close to -1 were obtained in log - log plots. Pit growth rates were higher for as-received sample (Fig. 4). For Al 2024, 6061 and 7075 exposed to 0.5 N NaCl it was found that b was close to -1 as shown in Table I which lists t_o and the fit parameters log a' and b. According to Eq. 1 with b = -1, pit growth rates are inversely proportional to exposure time [12]. It has to be noted that these measurements were carried under natural conditions, i.e. at E_{corr}, rather than at an applied potential exceeding the pitting potential. The pit growth law in Eq. 1 can be used to make lifetime predictions based on short-time laboratory investigations.

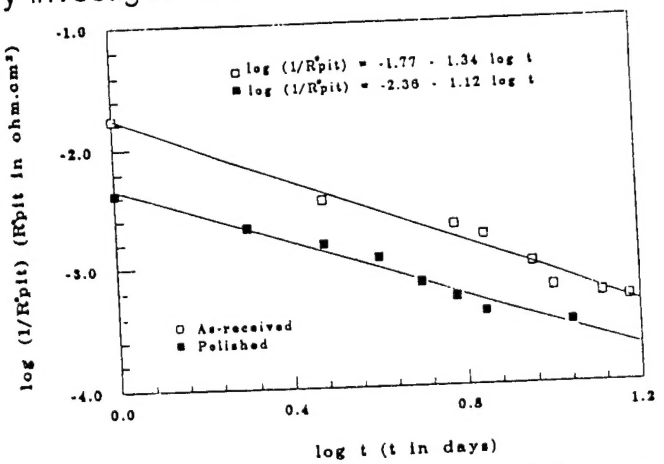

Fig. 4. Time dependence of $1/R^o_{pit}$ for untreated (as-received vs. polished) Al 6061 exposed to 0.5 N NaCl

Table I Parameters log a', b and t_0 in pit growth law for Al alloys

Alloy	log a'	b	t_o (days)
Al 7075-T6/passivated in $CeCl_3$	-3.00	-0.99	>25
Al 7075-T6/polished	-1.50	-1.35	≤ 1
Al 7075-T73/as-received	-1.93	-1.07	≤ 1
Al 7075-T73/deoxidized	-1.84	-1.11	≤ 1
Al 6061-T6/as-received	-1.77	-1.34	≤ 1
Al 6061-T6/polished	-2.36	-1.35	≤ 1
Al 6013-T6/as-received	-1.89	-0.86	≤ 1
Al 6013-T6/modified by Ce-Mo	-2.28	-1.25	>30

Electrochemical noise data have been obtained in the time domain as potential and current noise for an Al 2009/SiC MMC during exposure to 0.5 N NaCl (open to air). For comparison, noise data have also been collected for Pt in the same solution. Fig. 5a shows the potential noise data obtained during the first day of immersion during which pits initiated on the MMC which is very susceptible to localized corrosion. The noise data in Fig. 5 were normalized to remove the drift of the mean value during the measurement time. The potential noise fluctuations were of similar magnitude for both materials (Fig. 5a). However, the current noise were very large for the MMC and very small for Pt (Fig. 5b). The potential noise fluctuations for Pt, which is inert and has a poorly biased open-circuit potential, are considered due to minor changes in the mass transport conditions during the measurement. Obviously, only the current noise fluctuations are uniquely related to corrosion phenomena. The experimental data in Fig. 5 have been analyzed using power spectral density (PSD) plots. For the potential noise data similar dc limits were observed in the PSD plots for both materials (Fig. 6a). The slope in the linear region of the PSD plot was about - 20 dB for the MMC, while a more complicated frequency dependence was observed for Pt. In the current PSD plot the dc limit was very low and close to the background noise of the potentiostat for Pt, while it was very high for the MMC. The slope in the linear region for the MMC was about - 15 dB. These results show that measurements of potential noise alone can be misleading in terms of evaluation of the (localized) corrosion behavior.

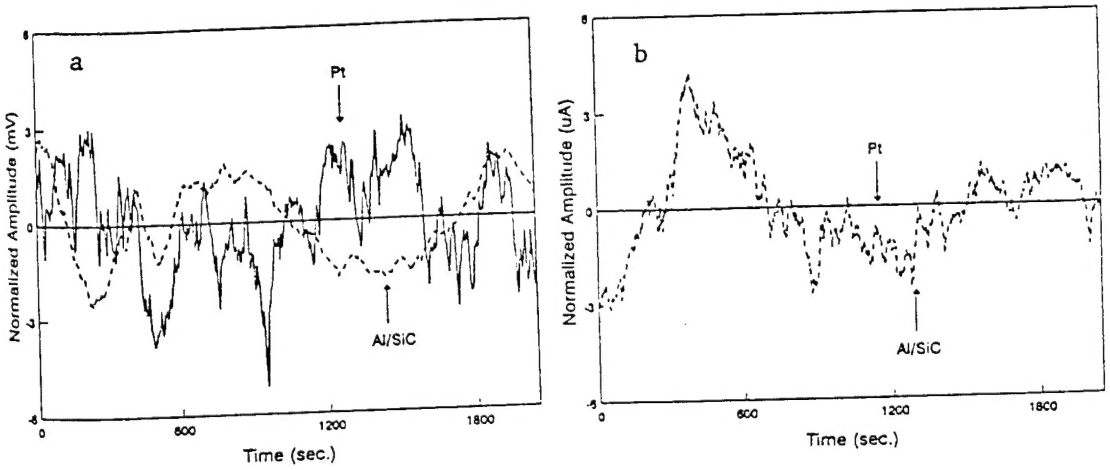

5. Normalized potential noise (Fig. 5a) and current noise (Fig. 5b) data for an Al 2029/SiC MMC and Pt exposed to 0.5 N NaCl.

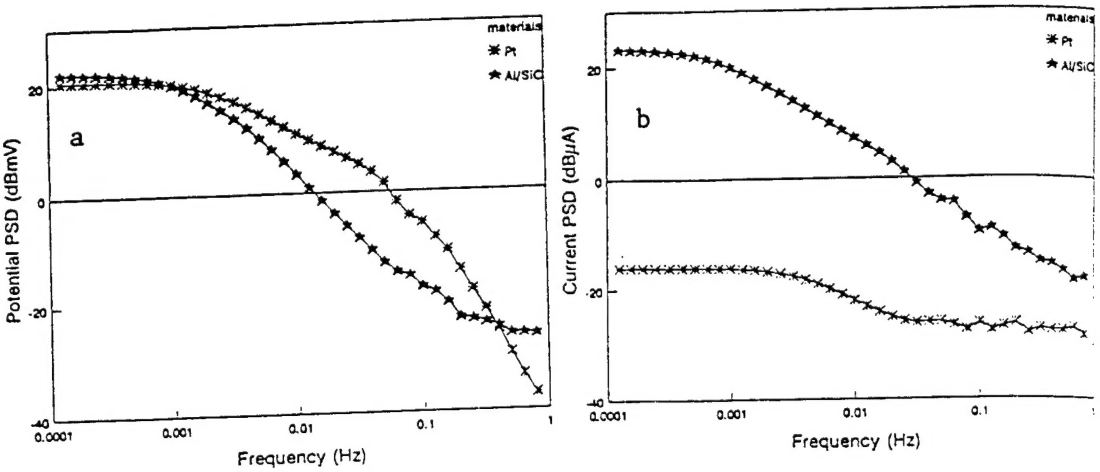

6. Potential (Fig. 6a) and current (Fig. 6b) PSD plots for Al 2009/SiC MMC and Pt exposed to 0.5 N NaCl (data of Fig. 5)

Fig. 7 shows potential and current PSD plots for the Al 2009/SiC MMC exposed to 0.5 N NaCl for 14 days. The potential PSD plots did not change much with exposure time (Fig. 7a). A dc limit was observed at the lowest frequencies and a linear portion in the PSD plots at higher frequencies with a slope of about - 20 dB was found for all exposure times. The current PSD plots displayed essentially the same features, however the dc limit, which is considered to be related to the intensity of localized attack, decreased sharply after one day and the slope was about -15 dB (Fig. 7b). The results from the current noise data agree with the observation based on EIS data that for this MMC pitting is severe in the earliest stages of exposure, but decreases in intensity with time. Attempts to correlate the characteristic parameters of the PSD plots such as dc limit, roll-of frequency and slope (Fig. 6 and 7) with the rate and type of the corrosion reaction have been made [13]. In addition, the noise resistance R_n defined as the ratio of the standard deviation of potential and current noise data has been used to follow the time dependence of localized corrosion processes for Al alloys and Al-based MMCs.

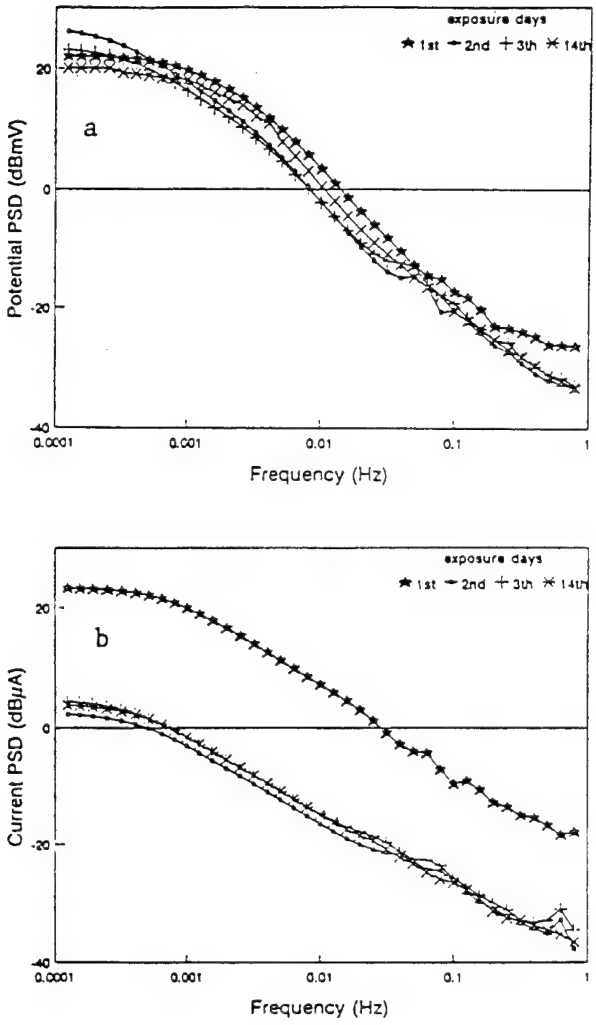

Fig. 7. Potential (Fig. 7a) and current (Fig. 7b) PSD plots for Al 2009/SiC MMC exposed to 0.5 N NaCl for 14 days.

2. Iron Exposed to NaCl Solutions of Different Corrosivity

This model system has been used to evaluate the relationship of R_p determined by EIS with the noise resistance R_n obtained from ENA [7,8]. The noise resistance R_n is defined as the ratio of the standard deviation of the potential fluctuations ($\sigma\{V(t)\}$) and the standard deviation of the current fluctuations ($\sigma\{I(t)\}$) determined from electrochemical noise data [13]:

$$R_n = \sigma\{V(t)\}/ \sigma\{I(t)\} \qquad (3)$$

Fig 8 shows the time dependence of the mean values of E_{corr}, while the mean values of the coupling current are plotted in Fig. 9 for pure iron exposed to 0.5 N NaCl which was saturated with air, deaerated or contained 10 mM $NaNO_2$ as inhibitor. E_{corr} was measured vs. a reference electrode (SCE) as the potential of two iron electrodes connected to a potentiostat which acted as a ZRA, while the coupling current between the two electrodes was measured at the potentiostat

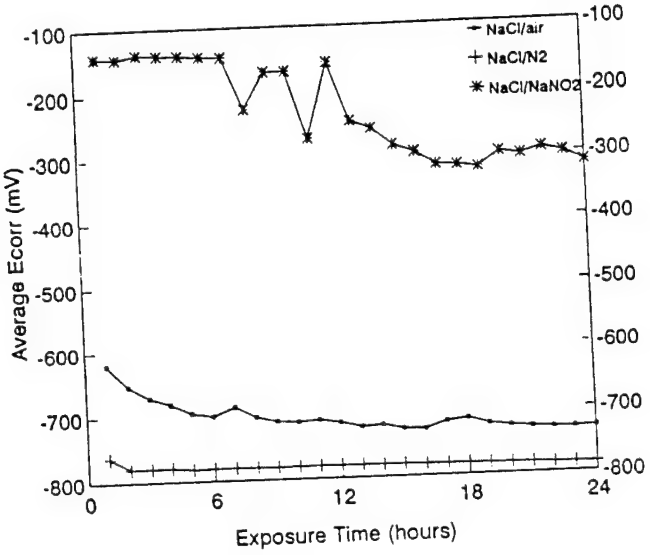

Fig. 8. Time dependence of the mean value of E_{corr} for iron exposed to solutions of different corrosivity.

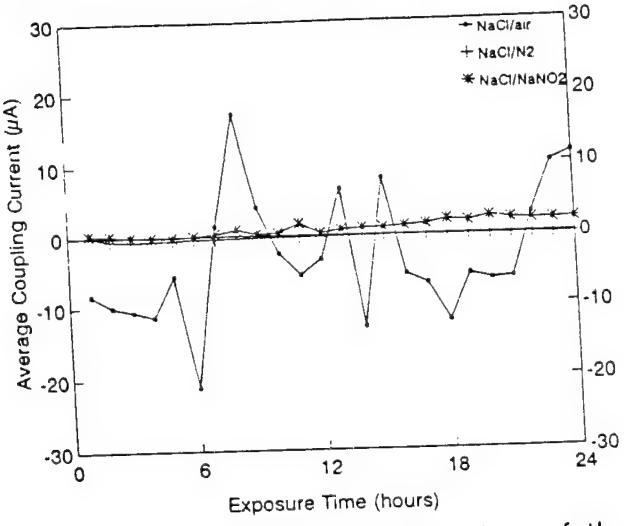

Fig. 9. Time dependence of the mean value of the coupling current for iron exposed to solutions of different corrosivity.

output [7,8]. The $\sigma\{V(t)\}$ and $\sigma\{I(t)\}$) data are plotted as a function of exposure time in Fig. 10 and 11, respectively. The time dependence of R_n determined according to Eq. 3 is shown in Fig. 12. R_n had the highest values for the inhibited solution and the lowest values with the most pronounced fluctuations for the NaCl solution open to air. It will be noted that the values of $\sigma\{V(t)\}$ (Fig. 10) are the highest for the solution with the lowest corrosivity (Fig. 12) for which very low values of $\sigma\{I(t)\}$ were recorded. This result shows again that potential noise data alone cannot be used to determine corrosion kinetics and mechanisms.

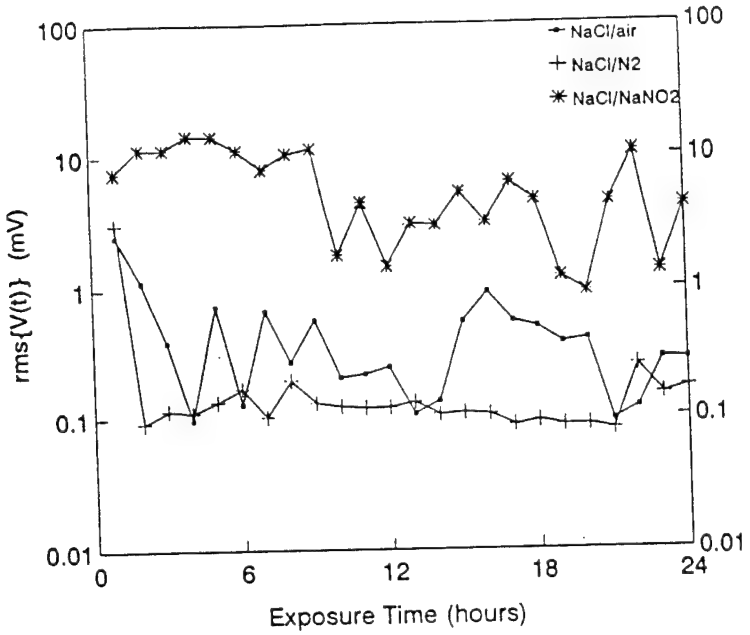

Fig. 10. Time dependence of $\sigma\{V(t)\}$ for iron exposed to solutions of different corrosivity.

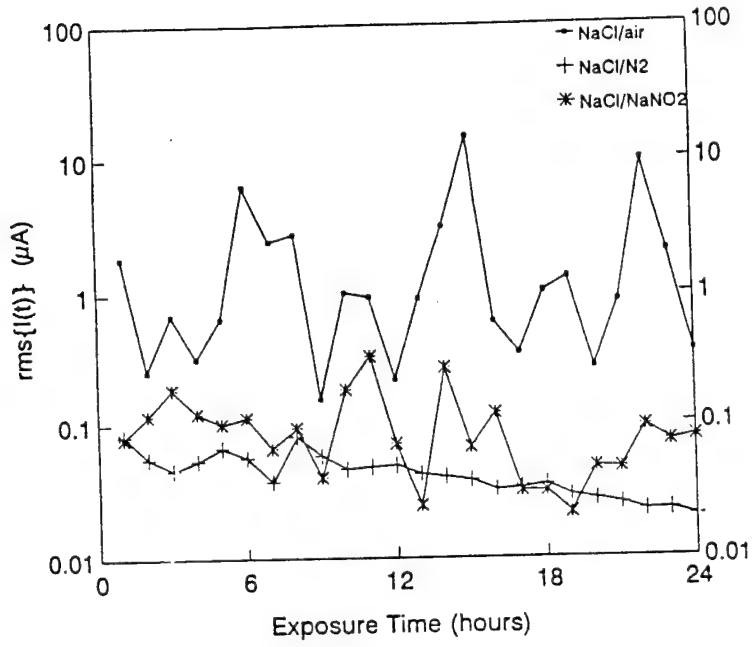

Fig. 11. Time dependence of $\sigma\{I(t)\}$ for iron exposed to solutions of different corrosivity.

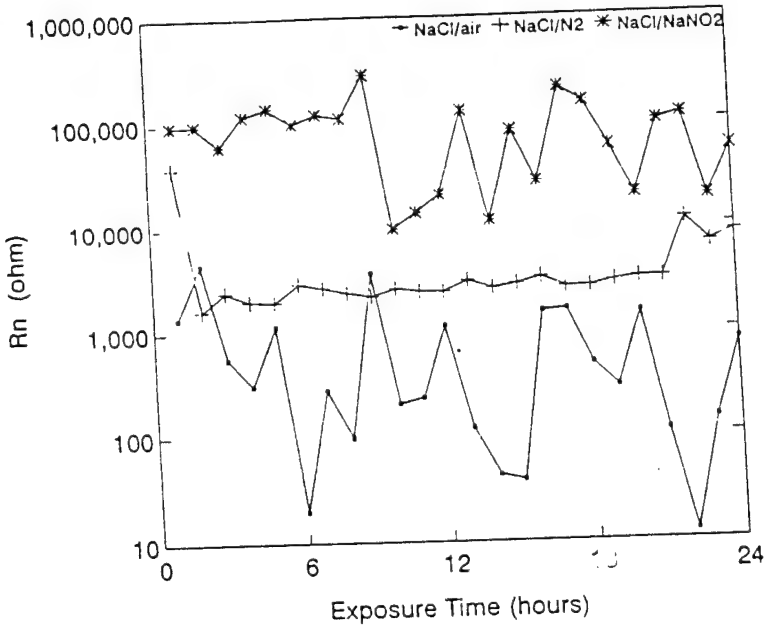

Fig. 12. Time dependence of noise resistance R_n for iron exposed to solutions of different corrosivity

At the end of the 24 hour exposure time EIS data were obtained for the three systems. From these data the polarization resistance R_p was obtained by fitting to a simple one-time-constant model. Satisfactory agreement between R_p and R_n was observed (Table II).

Table II. Comparison of R_n and R_p for three different test environments

	open to air	deaerated (N_2)	inhibited ($NaNO_2$)
R_n(KΩ)	0.8	8.3	54.7
R_p(KΩ)	1.6	15.9	22.1

Recently, a new experimental approach has been introduced which allows simultaneous collection of potential and current noise [7,8]. From these data R_n can be obtained, but it is also possible to construct noise spectra in which the spectral noise data are plotted as a function of frequency after transformation of the experimental data from the time domain into the frequency domain using FFT. The ratio $R_{sn} = V(f)/I(f)$ of the values for potential V(f) and current noise I(f) at each frequency is recorded from which the spectral noise resistance R^o_{sn} can be determined as the limit of $R_{sn}(f)$ for zero frequency:

$$R^o_{sn} = \lim_{f \to 0} \{R_{sn}\} \qquad (4).$$

Fig. 13 shows noise spectra for iron exposed for 1 and 24 h to NaCl with and without $NaNO_2$. For the uninhibited solution R_{sn} is low and independent of frequency, while for the inhibited solution a slope close to -0.5 is observed. A comparison of R_p, R_n and R^o_{sn} is given in Table III for the two solutions. Satisfactory agreement between R_p obtained from EIS and R_n and R^o_{sn} obtained from ENA is observed. It has to be emphasized that a theoretical analysis of the relationship of R_n and R^o_{sn} to R_p and (localized) corrosion rates does seem not exist at present.

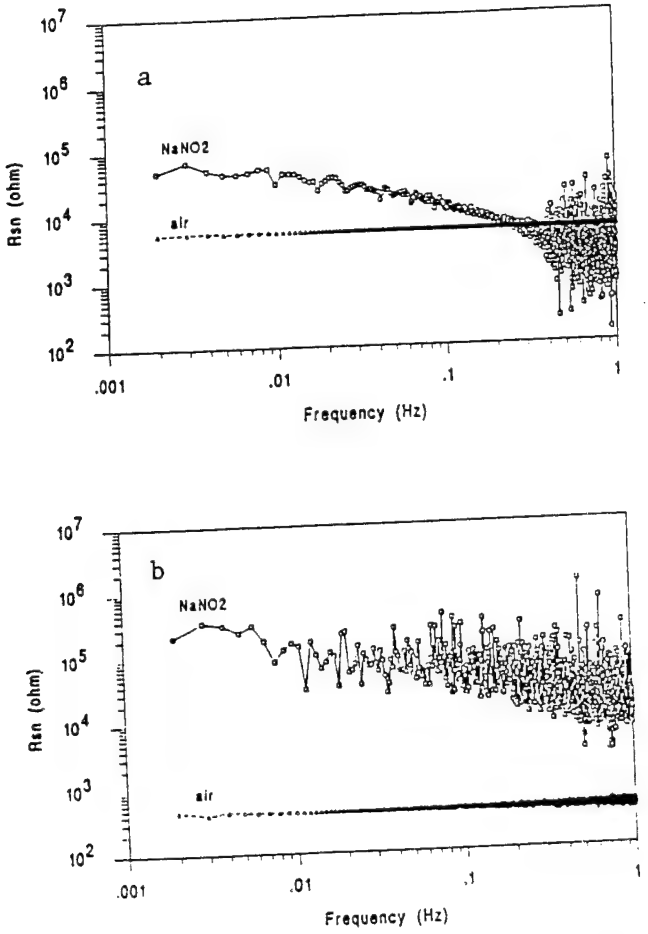

Fig. 13. Noise spectra for iron exposed to 0.5 N NaCl (open to air) with and without 10 mM $NaNO_2$ for 1 h (Fig. 13a) and 24 h (Fig. 13b).

Table III. Comparison of R_n, R^o_{sn} and R_p for simultaneously recorded noise data

	open to air	inhibited ($NaNO_2$)
$R_n(K\Omega)$	0.4	195.8
$R^\circ_{sn}(K\Omega)$	0.4	79.1
$R_p(K\Omega)$	1.4	220.0

3. Polymer Coatings on Steel

One of the most successful applications of EIS is the evaluation of the properties of polymer coatings on metals and their degradation with exposure time to corrosive environments which leads to corrosion at the metal/coating interface [4,5]. Mansfeld and Tsai [5,15,16] have shown that the fit parameters obtained for the coating model or certain parameters measured in the high-frequency region can be used to monitor coating degradation. For an alkyd system (CR 2) on cold-rolled steel exposed to 0.5 N NaCl, it was shown that initially the main degradation process was disbonding of the coating, while at longer exposure times the coating resistivity decreased as conducting paths developed [5,16,17]. Fig. 14 shows the time dependence of the delamination ratio $D = A_d/A$, where A_d is the delaminated area and A the total area, calculated as the average value from three parameters (C_{dl}, f_b/f_{min} and Φ_{min}) obtained from the analysis of the impedance spectra in Fig. 15 [5,17]. These parameters are identified in the model for polymer coatings and a theoretical impedance plot in Fig. 16. It was assumed that $D = 10^{-4}$ after 32 days. D increased by a factor of thirty during immersion for four months. In Fig. 17, the parameter $f_b/(f_{min})^2 = 2\pi d\rho C^o_{dl} = k\rho$ is plotted which can be used to determine changes of the coating resistivity ρ assuming that the coating thickness d and the specific double layer capacitance C^o_{dl} remain constant during exposure. For $d = 25\ \mu m$ and $C^o_{dl} = 30\ \mu F/cm^2$ a decrease of ρ from about 2.10^{10} ohm.cm to 3.10^7 ohm.cm is estimated between one and five months exposure for CR 2 [5,17]. These results demonstrate that EIS is capable of detecting localized corrosion phenomena such as disbonding of the coating and initiation of corrosion at the metal coating/interface as well as deterioration of the polymer coating and loss of its protective properties.

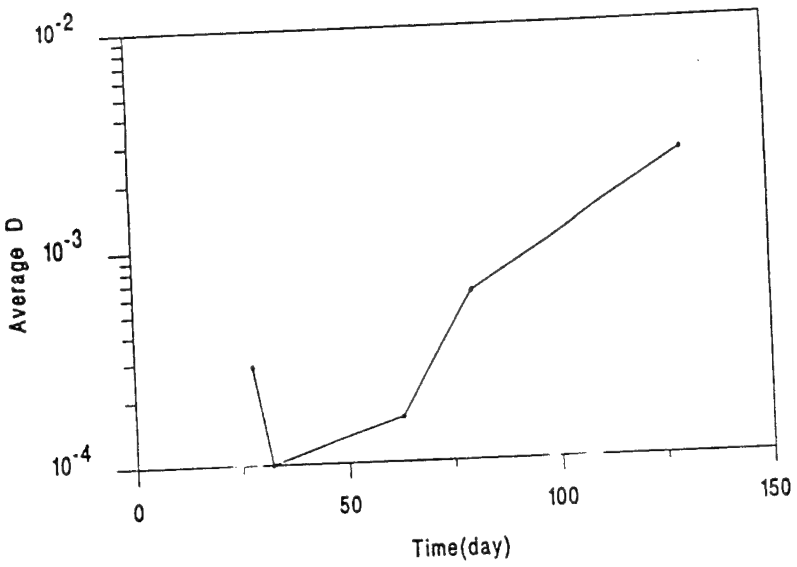

Fig. 14. Time dependence of the averaged delamination ratio D for coating system CR 2 exposed to 0.5 N NaCl (open to air)

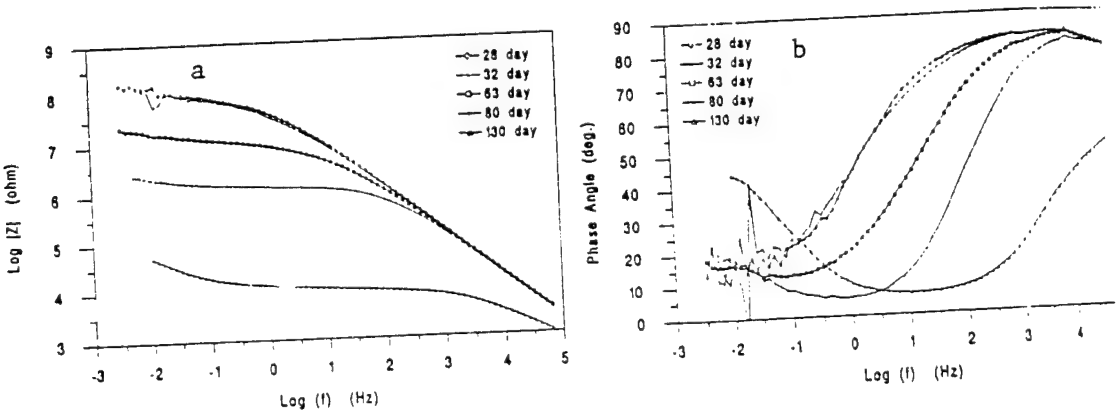

Fig. 15. Bode plots for CR 2 during exposure to 0.5 N NaCl

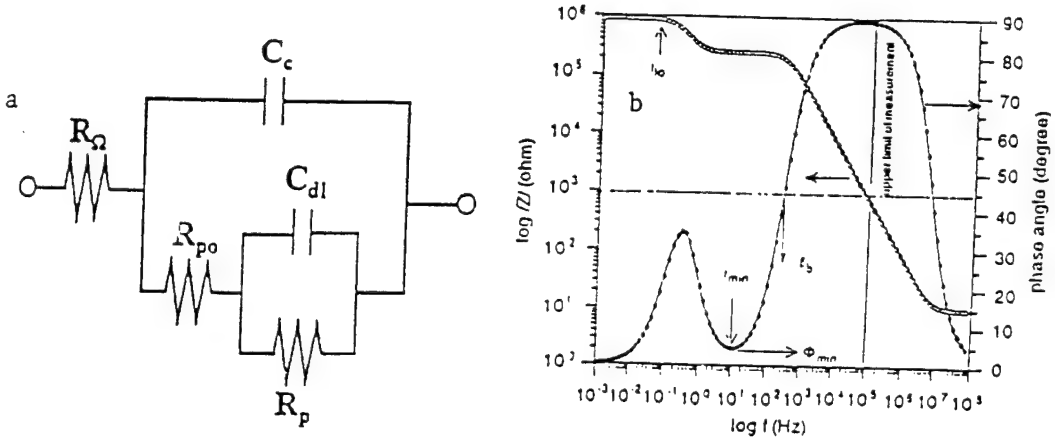

Fig. 16. Model for impedance of polymer coated steel (Fig. 16a) and theoretical impedance plot (Fig. 16b)

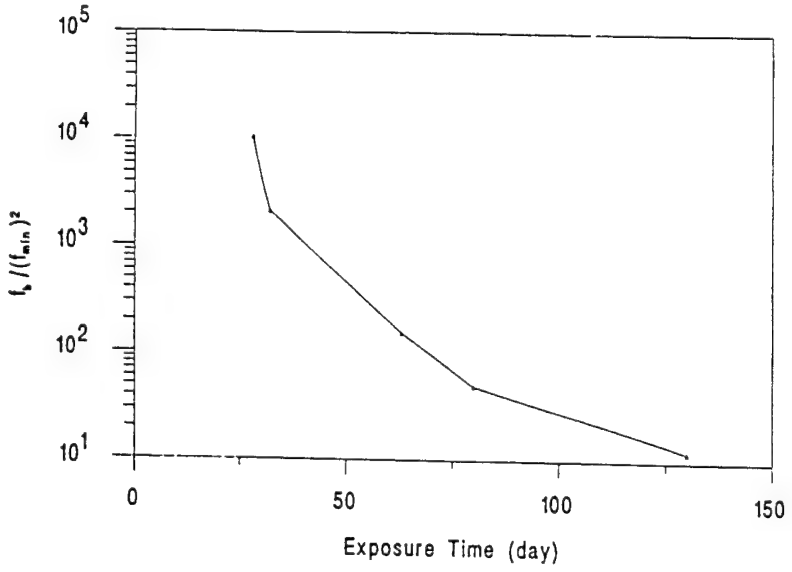

Fig. 17. Time dependence of $f_b/(f_{min})^2$ for coating system CR 2 exposed to 0.5 N NaCl.

The same coating system has been studied with ENA [17]. Fig. 18 shows a comparison of experimental potential (Fig. 18a) and current (Fig. 18b) noise data for CR 2 at exposure times of 28 and 130 days. It can be seen that the potential fluctuations for this less protective coating are much larger in the early stages of exposure than at longer times (Fig. 18a). On the other hand, the current fluctuations are much smaller on the 28th day than on the 130th day of exposure (Fig. 18b). This qualitative evaluation of noise data shows that potential noise levels decrease and current levels increase as the coating degrades. Similar observations were made by Skerry et al [14]. For the more protective epoxy polyamide coating (CR 9) no systematic changes of the noise levels with time were observed [17].

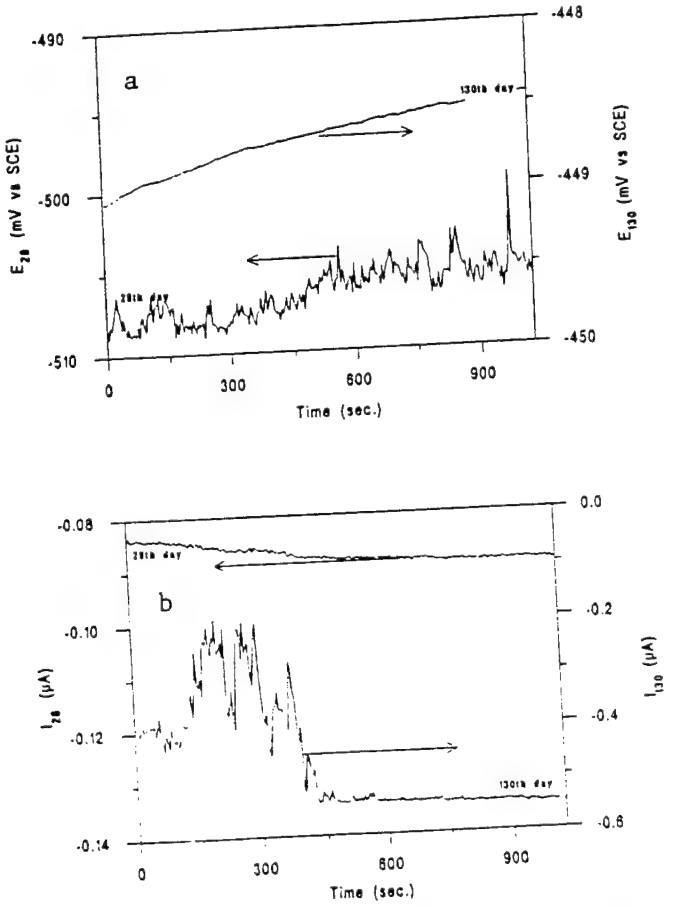

Fig. 18. Experimental potential (Fig. 18a) and current noise data (Fig. 18b) for coating system CR 2 after 28 and 130 days exposure to 0.5 N NaCl.

Noise spectra for the alkyd coating (CR 2) and the epoxy coating (CR 9) after exposure for 28 and 130 days are shown in Fig. 19. In all cases R_{sn} is independent of frequency with higher values for CR 9 for which no indication of deterioration and/or loss of corrosion protection was observed. The resistive parameters obtained from statistical and spectral noise analysis are plotted in Fig. 20. For CR 2 R_n and R^o_{sn} decreased with time, while for CR 9, R_n and R^o_{sn} remained at much higher values and did not change significantly with time indicating that degradation of the coating had not occurred in agreement with previous observations [5,16].

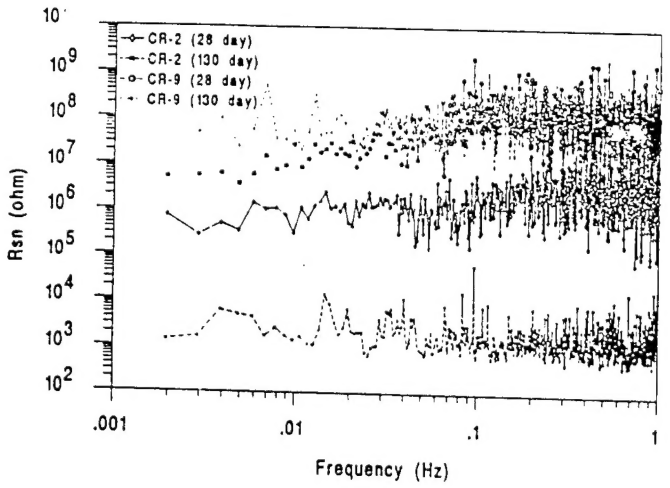

Fig. 19. Spectral noise plots for coating systems CR 2 and CR 9 after exposure to 0.5 N NaCl for 28 and 130 days.

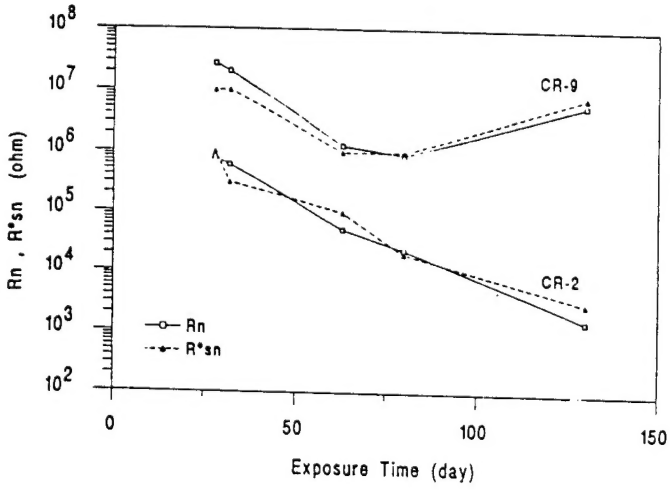

Fig. 20. Time dependence of R_n and R^o_{sn} for CR 2 and CR 9.

In Fig. 21 the same time dependence of R_n and R^o_{sn} obtained from ENA and R_p and R_{po} obtained from EIS is observed. The numerical values of R_n and R^o_{sn} are very similar, but much lower than those of R_{po} and R_p. A comparison of the results obtained with EIS and ENA suggests that more detailed information concerning loss of corrosion protection with time can be obtained from EIS by analyzing the changes of individual fit parameters such as C_c, R_{po}, R_p and C_{dl} using known correlations of these parameters with water-uptake of the coating, decrease of coating resistivity and increase of the delaminated area, respectively [5,15,16].

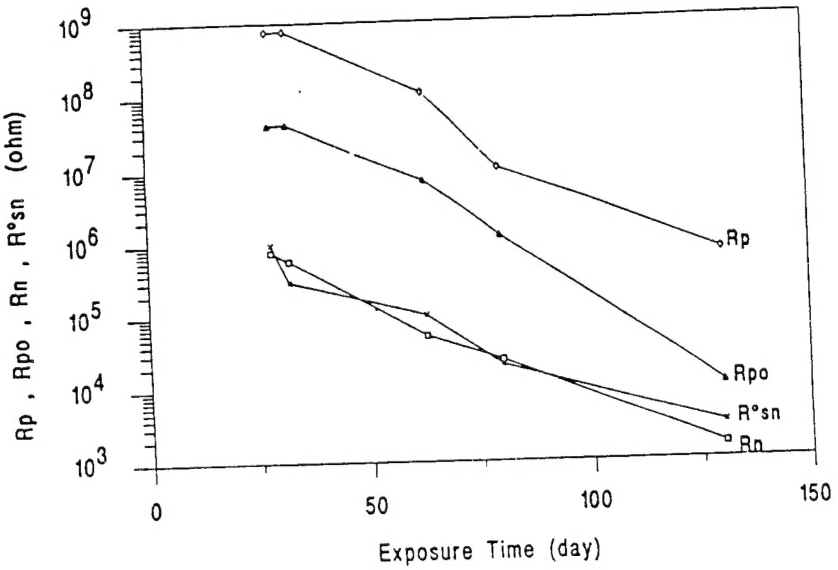

Fig. 21. Time dependence of R_p, R_{po}, R_n and R^o_{sn} for coating system CR 2 exposed to 0.5 N NaCl

The coatings CR 2 and 9 together with 10 other coating systems will be evaluated further in a joint project with J. Jones-Meehan and B. Little during exposure to natural seawater in Port Hueneme, California and Ft. Lauderdale, Florida and to artificial seawater. EIS and ENA data will collected over six months periods using the techniques described above. After exposure samples will be evaluated with the environmental SEM (ESEM) by B. Little and co-workers to determine the structure of the biofilm, location of bacteria and damage to the polymer coating. Samples exposed by J. Jones-Meehan and co-workers to different

colonies of bacteria will be evaluated by EIS to determine changes of coating properties and the extent of corrosion at the metal/coating interface and by ESEM.

Summary and Conclusions

Both EIS and ENA can be used to obtain important kinetic information for different corrosion systems. At the present state of our understanding of ENA it seems that more detailed information can be derived from EIS data which are collected in a very wide frequency range. This conclusion has been reached from the analysis of EIS and ENA data for three different systems: Al/NaCl Fe/NaCl and polymer coated steel/NaCl. Analysis of EIS data for polymer coated metals allows estimation of water uptake of the coating from the increase of C_c with time, decrease of coating resistivity, degree of disbonding of the coating and initiation of corrosion at the metal/coating interface based on the parameters shown in Fig. 16a and b. Electrochemical noise data are typically observed only for $f < 1$ Hz as shown for the three examples presented here. Analysis of noise data by statistical methods results in R_n, while from spectral analysis R^o_{sn} can be obtained. While R_n and R^o_{sn} have shown similar changes with time as R_p and R_{po} for a polymer coating with relatively poor performance, their numerical values are much lower than those of R_{po} and R_p. Both R_n and R^o_{sn} remained at much higher values for the coating with excellent performance than for the coating with poorer performance.

The advantages of ENA are the low cost of equipment and the relatively simple methods for data collection which makes this method very attractive for corrosion monitoring. A disadvantage at present seems to be the difficulty of data interpretation. Further research concerning the correlation of potential and current noise with different phenomena occurring during localized corrosion is needed. Eventually, the main application of ENA might be found in corrosion monitoring using the simple statistical approach leading to R_n or more complicated analyses in the frequency domain in the form of PSD plots resulting in parameters related to corrosion phenomena or of spectral noise analysis leading to R^o_{sn}.

More information concerning the application of EIS and ENA to MIC will become available in a project funded by the Office of Naval Research in which 12 different polymer coating systems will be exposed to natural seawater for six months periods at two locations and to

different colonies of bacteria. The experimental approach to be taken will be similar to that described above.

References

1. F. Mansfeld, S. Lin, S. Kim and H. Shih, J. Electrochem. Soc. 137, 78 (1990)
2. F. Mansfeld, S. Lin, S. Kim and H. Shih, Electrochim. Acta 34, 1123 (1989)
3. F. Mansfeld and B. Little, Corr. Sci. 32, 247 (1991)
4. F. Mansfeld and W. J. Lorenz, in "Techniques for Characterization of Electrodes and Electrochemical Processes", J. Wiley, 1991, p. 581 - 647
5. F. Mansfeld, "The Use of EIS for the Study of Corrosion Protection by Polymer Coatings - A Review", submitted to J. Appl. Electrochem.
6. F. Mansfeld, H. Shih, H. Greene and C. H. Tsai, ASTM STP 1188, 37 (1993)
7. F. Mansfeld and H. Xiao, J. Electrochem. Soc. 140, 2205 (1993)
8. F. Mansfeld and H. Xiao, Proc.12th Int. Corrosion Congress, Houston, TX, Sept. 1993, p. 1388
9. F. Mansfeld, Y. Wang, S. H. Lin, H. Xiao and H. Shih, ASTM STP 1188, 297 (1993)
10. F. Mansfeld, H. Shih and Y. Wang, J. Electrochem. Soc. 138, L74 (1991)
11. F. Mansfeld, Y. Wang and H. Shih, Electrochim. Acta 37, 2277 (1992)
12. F. Mansfeld, Y. Wang, H. Xiao and H. Shih, in Proc. "Critical Factors in Localized Corrosion", The Electrochem. Soc., Proc. Vol. 92-9, p. 469 (1992)
13. F. Mansfeld and H. Xiao, in Proc. Symp. "Biofouling and Biocorrosion in Industrial Water Systems", ACS, Washington, D.C., August 1992, Lewis Publ. (in press)
14. B. S. Skerry and D. A. Eden, Prog. Org. Coat. 15, 269 (1987); B. S. Skerry, A. Alavi and K. I. Lindgren, J, Coat. Techn. 60, 97 (1988); C. T. Chen and B. S. Skerry, Corrosion 47, 598 (1991)
15. F. Mansfeld and C. H. Tsai, Corrosion 47, 958 (1991)
16. C. H. Tsai and F. Mansfeld, Corrosion 49, 726 (1993)
17. H. Xiao and F. Mansfeld, "Evaluation of Coating Degradation with EIS and ENA", J. Electrochem. Soc. (in press)